

CT Myelographic Findings in Degenerative Disorders of the Cervical Spine: Clinical Significance

L. Penning¹
J. T. Wilmink
H. H. van Woerden
E. Knol

CT myelographic data in 80 patients with clinical evidence of nerve-root involvement or long tract signs attributed to degenerative disorders of the cervical spine were classed into five diagnostic groups, and their clinical significance was assessed. Unilateral flattening of the cord by a spondylotic mass or bulging disk in a normally wide canal (group 1) was considered nonspecific because nerve-root signs were nearly as often contralateral as unilateral to the radiologic findings, and none of the patients had long tract signs. As a rule, conventional myelography showed only minor root-sleeve deformity. Concentric compression of the cord in a narrow (stenotic) canal (group 2) proved to produce long tract signs only after the cross-sectional area of the cord had been reduced by about 30% to a value of about 60 mm² or less. In most cases, nerve-root swelling (group 3) coincided with the side of nerve-root symptoms. A 100% correlation was found between the side of disk herniation with occlusion of the corresponding foramen (group 4) and the side of nerve-root symptoms. In 24 patients, cord and nerve roots showed no abnormalities (group 5). If stenosis of the spinal canal, nerve root swelling, and disk herniation are considered specific CT myelographic signs in nerve-root symptomatology, a specific diagnosis could be made in about 40% of the cases.

After preliminary experience with cervical CT myelography, we were impressed by the wealth of information this method offers relative to conventional myelography, but we had to register several obviously false-positive findings because clinical nerve-root symptoms were contralateral to the side of radiologic findings. It is already known from conventional myelography that root deformities correlate poorly with clinical symptomatology [1]. Recent CT myelographic studies, however, claim to compare favorably with conventional myelography in this respect [2-5]. Therefore, we decided to assess a series of CT myelographic studies in patients suspected of having nerve-root and/or cord involvement caused by degenerative disorders of the cervical spine and to compare the radiologic findings with the information provided by the clinician. Several CT myelographic features were assessed relative to clinical signs of nerve-root and cord involvement. The study focused, in patients with nerve-root signs, on identifying clearly false-positive radiologic signs, and, in patients with long tract signs, on establishing borderline values for reduction of cross-sectional area of the spinal cord.

Materials and Methods

We studied 80 CT myelograms. In half of the cases, conventional myelograms obtained with an aqueous contrast medium immediately before the CT investigation were available. CT was carried out with Tomoscan 310 machines in two separate locations (University Hospital and Roman Catholic Hospital, both at Groningen). Slice thickness varied from 1.5 to 3 mm, being taken 1.5 or 3 mm apart at the suspected disk levels and the adjoining vertebral portions (fig. 1). In most patients two or three levels were studied.

To gain insight into the diagnostic significance of various morphologic abnormalities, we

This article appears in the January/February 1986 issue of the *AJNR* and the April 1986 issue of the *AJR*.

Received May 1, 1985; accepted after revision August 14, 1985.

¹ All authors: Department of Neuroradiology, University Hospital, Postbus 30.001, 9700 RB Groningen, The Netherlands. Address reprint requests to L. Penning.

AJNR 7:119-127, January/February 1986
0195-6108/86/0701-0119

© American Society of Neuroradiology

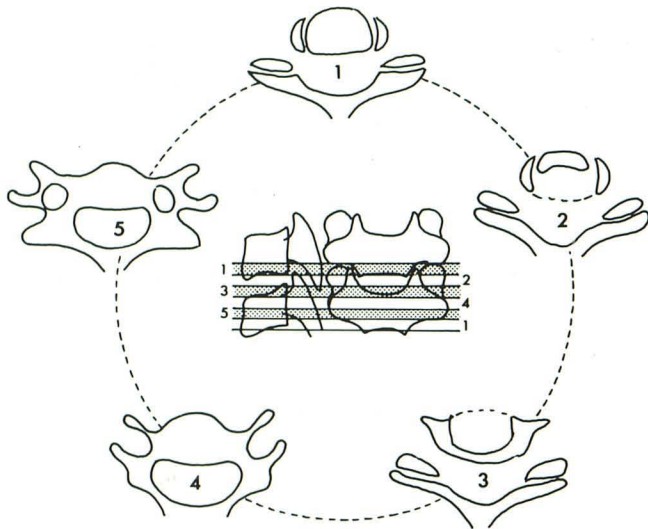


Fig. 1.—Levels of CT depiction. Central figure shows levels of CT investigation. Slice thickness in this example is about 3 mm, and five slices are necessary to cover height of one vertebra and disk. Slices 1–3 pass through intervertebral foramen and slices 4 and 5 through pedicle.

divided our findings into five radiodiagnostic groups: (1) cord deformation in a normally wide subarachnoid space (fig. 2); (2) cord deformation in a narrowed subarachnoid space (fig. 3); (3) nerve-root involvement as evidenced by local nerve-root swelling (fig. 4); (4) nerve-root involvement due to occlusion of the entrance of the intervertebral foramen (fig. 5); and (5) no cord or nerve-root involvement, however, dural indentations were frequently present (fig. 6).

Besides this morphologic assessment, measurements were made at the level of maximal abnormality (as a rule, at C5–C6; in group 5, all measurements were made at C5–C6): cross-sectional area of spinal cord; cross-sectional area of surrounding subarachnoid space; midsagittal diameter of dural sac; and ratio between midsagittal and transverse diameter of spinal cord.

Diameters and cross-sectional areas were computed by an independent CT viewing console after indicating the relevant landmarks or encircling the relevant area with a light pen on the display screen. Window width was routinely set at 800 H with levels usually centered around 200 H.

Cord deformation was defined as asymmetry of its cross-sectional shape, distortion into a trigonal or rhomboid form and/or flattening or rotation. At first, flattening was assessed visually, but after analysis of measurements it was decided that flattening should be defined as a ratio of midsagittal to transverse diameter less than 0.4. Likewise, narrowing of the subarachnoid space was initially assessed visually but later was defined as a cross-sectional area of less than 70 mm². The level with the smallest dimensions was always chosen as representative of the case.

Nerve-root swelling was defined as an increase in root diameter to at least twice normal at the area in question (fig. 4). As nerve roots are too small to make reliable measurements, nerve-root swelling was only assessed visually. Nerve-root involvement was assumed to be present in cases of complete occlusion of the subarachnoid space at the entrance of the intervertebral foramen (fig. 5). No assessment of bony narrowing of the intervertebral foramen was attempted.

Reliability of measurements was tested by measuring the cross-sectional area of the cord on 20 different CT images, repeating each measurement five times, and determining the maximal spread from

the mean value of the five measurements. If conventional myelograms were available, their findings were compared with those of CT myelography. Data on clinical symptoms of the patients were collected from the radiodiagnostic request forms. If necessary, extra information was obtained by consulting the referring physician.

Results

Group 1 comprised 16 patients. As a rule, cord deformation consisted of unilateral flattening of the cord with or without some rotation to the contralateral side. Anterior to the flattened part of the cord, bony encroachment extending partly or completely across was present at the anterior border of the spinal canal, lending the latter an asymmetric appearance (fig. 2). In three cases the mass was of a purely soft nature, giving the appearance of a unilaterally bulging disk (fig. 7). The mass sometimes narrowed the corresponding intervertebral foramen, but never occluded its entrance completely, thus leaving the root sleeve more or less indented but still opacified by the contrast medium.

Conventional myelograms were available in 13 cases. In one case anterior indentation of the dural sac was present at the disk levels; in another case anterior and posterior indentations were seen in extension. In a third case a bilateral root-sleeve defect was found due to the presence of swollen nerve roots. In the other cases the root sleeves on the myelograms had been judged as normal, but in retrospect occasional slight loss of density of the root sleeve involved on the CT myelogram could be detected (fig. 2).

Results of measurements on the cord and surrounding subarachnoid space are presented in table 1. Measurement error proved to remain below 3% in 75% of the cases and below 5% in 90%. Error was 7%–9% in 5% of the cases and never surpassed 9%.

Statistically significant differences between the different groups with regard to different measurements are presented in table 2. Analysis of variance of the data showed that group differences among means were highly significant. Therefore, Student *t* tests were performed to locate these differences. Table 2 shows the *p* values resulting from the *t* test.

Correlation with clinical findings revealed that in diagnostic group 1 no cases with long tract signs were present despite deformation of the cord. Clinical signs of nerve-root involvement were unilateral to the radiologic abnormality in seven cases, contralateral in six cases, and bilateral in two cases. In one case no cord or root signs were present.

Group 2 included 24 patients. As a rule, cord deformation took the form of a cross-sectional shape congruent with that of the spinal canal (fig. 3). In several cases the cord also was more or less rotated.

Conventional myelograms were available in 11 cases. A block in extension was found in eight cases; in one more case the "block" was unilateral. After restoration of flow of the contrast medium by cervical flexion, a permanent root-sleeve defect was detected in three cases. According to the CT myelographic findings, this defect resulted from the additional presence of a soft mass as defined in group 4 (these patients were also included in group 4).

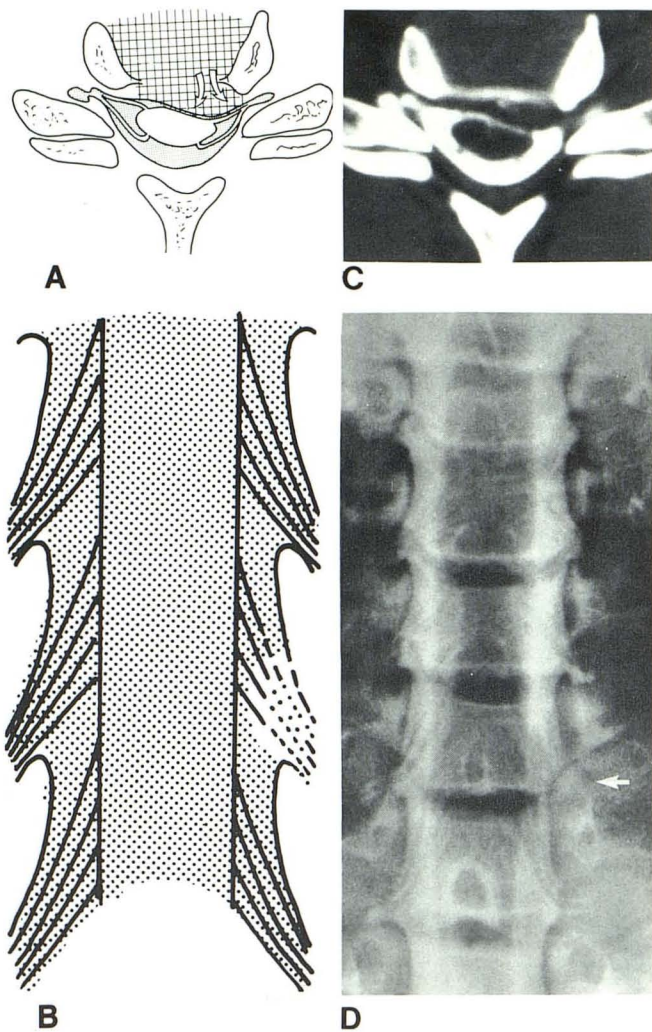


Fig. 2.—Radiographic findings in group 1. **A**, Schematic drawing of CT myelographic findings. Unilateral flattening and rotation of cord in front of unilateral mass on anterior border of spinal canal, partly bony, partly soft in nature, and not completely occluding entrance of foramen (root sleeve still visible). Roomy subarachnoid space. **B**, Drawing of conventional myelogram. Corresponding root sleeve shows only minor abnormalities. **C**, CT myelogram at C5–C6 in 36-year-old woman with long-standing neck pain radiating into right arm, contralateral to side of mass at anterior border of spinal canal. Root sleeves on both sides are filled; cord is flattened on left side and rotated. **D**, Conventional myelogram of same individual. Less of density of left-sided C5–C6 root sleeve (arrow).

Results of measurements are presented in table 1. To investigate correlation with clinical findings the group has been subdivided into 2A (long tract signs, 11 patients) and 2B (no long tract signs, but unilateral nerve-root involvement in 11, bilateral nerve root involvement in one, and no root involvement in one).

Group 3 consisted of 11 patients. In six, nerve-root swelling was the only CT myelographic abnormality. The CT myelograms in the other five cases showed, besides nerve-root swelling, a deformed cord in a normal subarachnoid space (one case), a deformed cord in narrowed subarachnoid space

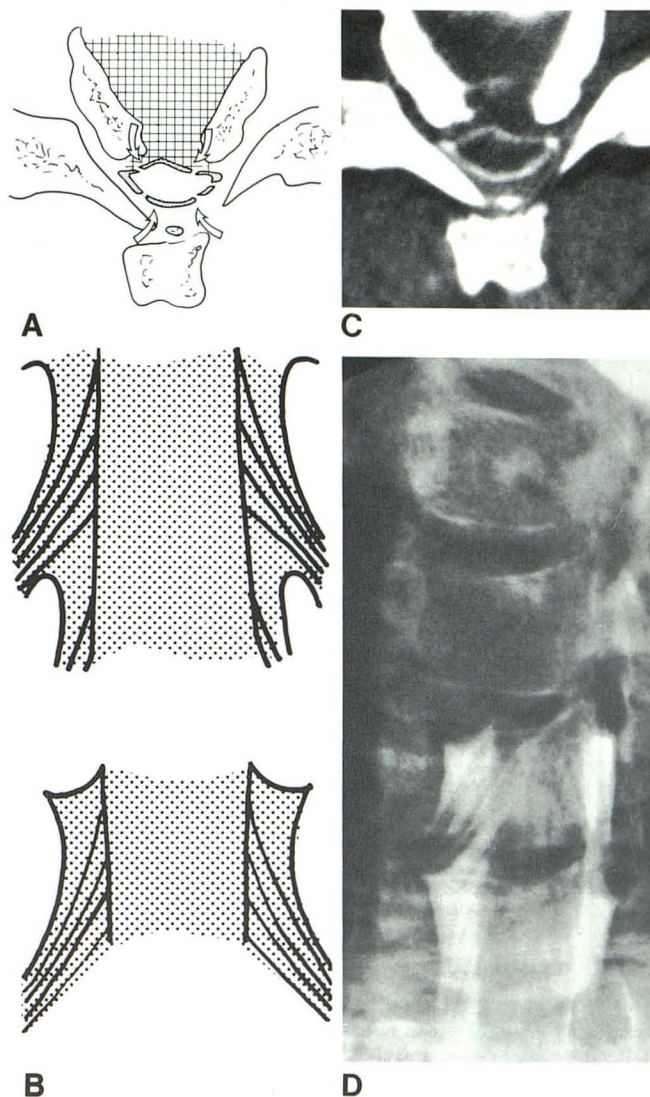


Fig. 3.—Radiographic findings in group 2. **A**, Schematic drawing of CT myelographic findings. Molding of spinal cord to shape of narrowed spinal canal. Narrow subarachnoid space with concentric encroachment on spinal cord by spondylotic deformations (arrows). **B**, Drawing of conventional myelogram. Block of flow of contrast medium in extension of cervical spine. **C**, CT myelogram in 49-year-old man with acute loss of strength in right hand and paresthesias. On extension of head, there were neck tingling sensations in both legs (patient was grouped as 2A). Marked narrowing of subarachnoid space and deformation of cord at C5–C6. **D**, Conventional myelogram, same patient. Block at C5–C6.

(one case), and an occluding mass at the entrance of the intervertebral foramen (three cases). Accordingly, these cases were also included in groups 1, 2, and 4, respectively. Nerve-root swelling manifested itself over an axial distance of some millimeters at the region of the lateral recess or entrance of the intervertebral foramen, and presented a rounded or barlike shadow occluding the recess nearly completely, simulating a diskogenic soft mass (fig. 4).

Conventional myelograms were available in seven cases. They demonstrated discrete, rounded defects within the cor-

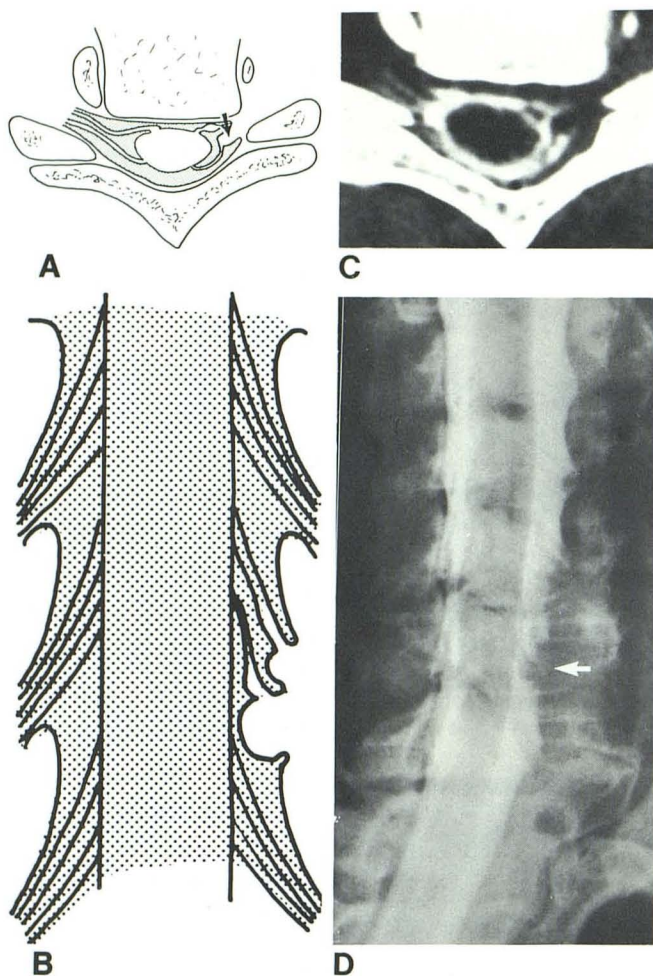


Fig. 4.—Radiographic findings in group 3. A, Schematic drawing of CT myelographic findings. Swelling of nerve root (*arrow*) at entrance of intervertebral foramen. More medially located part of nerve root is normal. B, Drawing of conventional myelogram. Rounded defects in corresponding root sleeve. C, CT myelogram at C6–C7 in 41-year-old woman with radiating pain in left arm and hand. Nerve-root swelling in region of entrance of left-sided intervertebral foramen. D, Conventional myelogram, same woman. Rounded defects in left-sided C6–C7 root sleeve (*arrow*).

responding root sleeves. In two cases, however, these defects were also present on the contralateral side, where the CT myelogram was normal. In two other cases the defect on the side of the abnormal root sleeve was larger and (according to the CT myelogram) attributable to the additional presence of a soft mass at the entrance of the foramen.

Nerve-root swelling corresponded to the side of clinical nerve-root involvement in nine cases, although in two instances nerve-root symptoms were bilateral. In the two other cases nerve-root swelling was bilateral, but clinical symptoms were unilateral.

Group 4 included 11 patients. The occluding mass invariably was of a soft nature and always had a topographic relation to the intervertebral disk. Often the mass extended downward alongside the pedicle of the vertebra below. In one case it extended slightly upward. A swollen nerve root was present

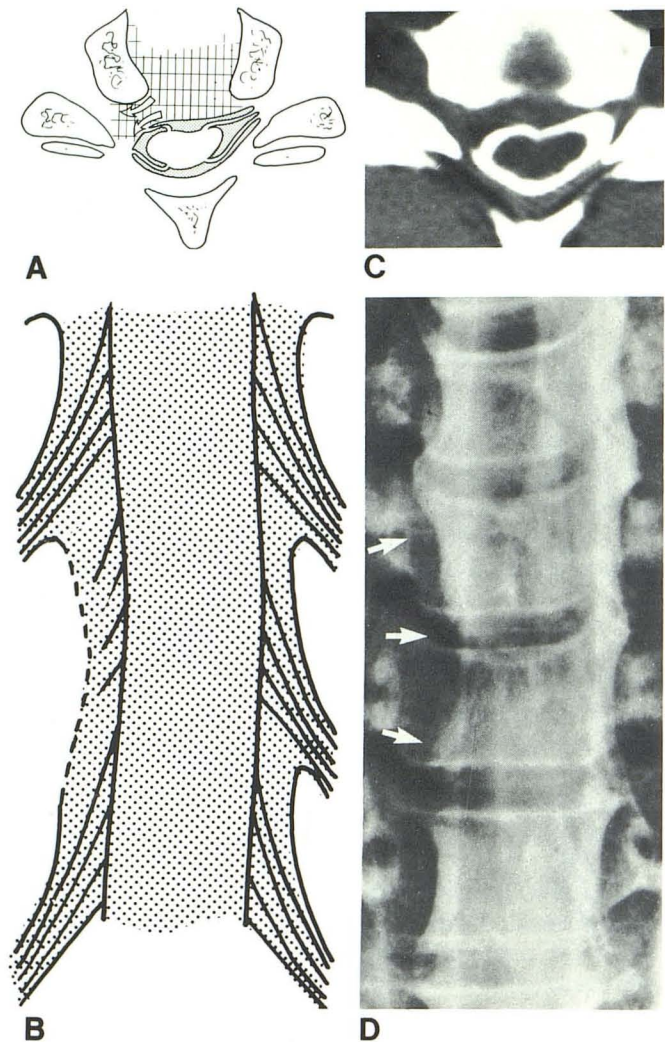


Fig. 5.—Radiographic findings in group 4. A, Schematic drawing of CT myelographic findings. Soft mass at entrance of intervertebral foramen (*arrows*). Complete amputation of filling of root sleeve. Deformation and rotation of cord. B, Drawing of conventional myelogram. Large defect at corresponding root sleeve with slight indentation of dural sac and slight displacement of cord. C, CT myelogram at C5–C6 in 41-year-old woman with neck pain radiating into right shoulder and arm, of some months duration. Soft mass at entrance of intervertebral foramen on right side, completely amputating corresponding root sleeve. D, Conventional myelogram before CT study. Large defect at site of right-sided C5–C6 root sleeve with slight indentation of dura above and below (*arrows*).

at the corresponding level in three cases (these cases have also been included in group 3). In five cases the mass also caused marked narrowing of the subarachnoid space, two such cases having long tract signs (these cases have also been included in group 2).

Conventional myelograms were available in nine cases. They showed a large defect at the site of the corresponding root sleeve in eight cases, with inward bulging of the dura above and/or below the defect. In addition, a block in extension was found in two of these cases, being unilateral at the side of the mass in one. In one case the defect at the site of

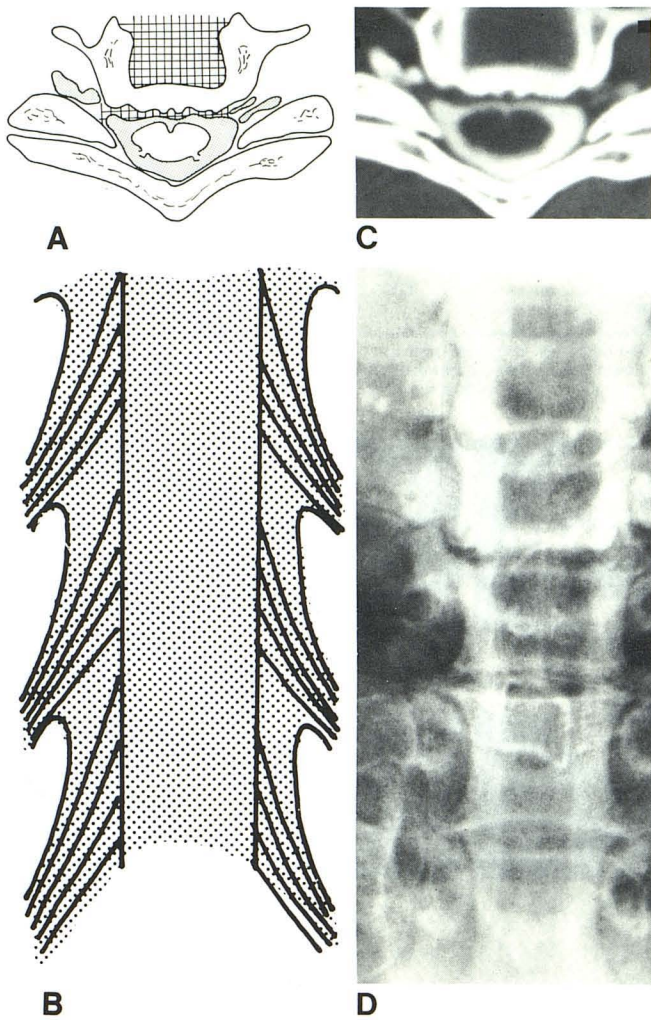


Fig. 6.—Radiographic findings in group 5. A, Schematic drawing of CT myelographic findings. Normal aspect of cord; no nerve-root swelling, irregular anterior dural contour due to osteophyte formation at posterior vertebral border, but no narrowed subarachnoid space. B, Drawing of conventional myelogram. Normal aspect of cord and roots. C, CT myelogram at C5-C6 in 58-year-old woman with pain radiating into left arm. Level is normal except for irregular anterior dural surface due to osteophyte formation. D, Conventional myelogram before CT study. Normal aspect of cord and root sleeves.

the mass was small. Correlation with clinical findings showed agreement in all cases between side of clinical nerve-root compression and side of occluding mass.

Group 5 comprised 28 patients. The CT myelograms were normal in 14 patients, apart from occasional minor spondylotic deformity. In the other cases marked bilateral spondylotic encroachment (unilateral in one case) on the anterior border of the spinal canal was present. In one case the subarachnoid space was narrowed.

Conventional myelograms were available in seven cases. They were invariably judged as normal. No significance was attached to the minor asymmetry of filling of root sleeves and anterior dural indentations present in some cases.

Results of measurements are presented in table 1. To investigate the influence of anterior spondylotic encroach-

ment, the mean values of the group with normal CT myelograms and those of the group with marked spondylosis were determined separately. No difference was found.

Clinical symptoms in group 5 were unilateral signs of nerve-root involvement (18 patients), bilateral nerve-root involvement (four patients), long tract signs (three patients), and other symptoms (three patients). In the 11 cases with marked anterior spondylosis, signs of nerve-root involvement were unilateral in 10 patients and bilateral in one. In the case with unilateral spondylotic encroachment (as in group 1), nerve-root symptoms were bilateral.

Discussion

Recent literature reports have attempted to assess the diagnostic accuracy of CT myelography on the basis of surgical verification [4, 5, 7]. This method has two distinct disadvantages: First, although the surgeon can confirm or disprove in most cases the radiologic assessment of the *anatomic* situation within the spinal canal, he is no more able than the radiologist to state with certainty that the patient's symptoms are *etiologically* related to the existing anatomic situation (bulging or herniated disk, bony spur, narrow canal). In other words, both the radiologist and the surgeon are describing the same morphologic features, and the correlation between the two techniques in the cervical spinal region is gratifyingly high. However, neither can tell us whether the features perceived are symptomatic or asymptomatic. The results of the operation (success or failure in relief of symptoms) can provide an indication in this direction, but they are by no means conclusive [8]. Second, selecting patients on the basis of having undergone surgery excludes patients with a discrepancy between clinical and radiologic findings, as was present in our group, and who will not undergo surgery.

Our method of comparing CT myelographic findings with clinical signs also has its limitations. Clinical symptomatology in general is insufficiently reliable to ascertain unequivocally the location of nerve-root involvement. Accordingly, attention was only paid to the side of nerve-root complaints, and no speculation was made as to the level. Therefore, if clinical symptomatology pointed to the side contralateral to the radiologic findings, these findings were considered false positive. If clinical and radiologic signs pointed to the same side, correlation was considered probable, although it is known that brachialgia can be produced by nerve-root compression as well as by a great variety of pathologic processes. Therefore, our method is more reliable for assessing false-positive results than for establishing a true-positive relationship. True- and false-negative findings are, of course, even more difficult to identify.

In group 1 (cord deformation in a normally wide subarachnoid space) radiologic signs were almost as often in disagreement as in agreement with the side of clinical signs. If this were to imply an almost random distribution, a causal relation between the anatomic and the clinical picture would seem unlikely, even in cases where both are on the same side. In the latter case, however, absence of a causal relation cannot be established with certainty either. Therefore, it seems more

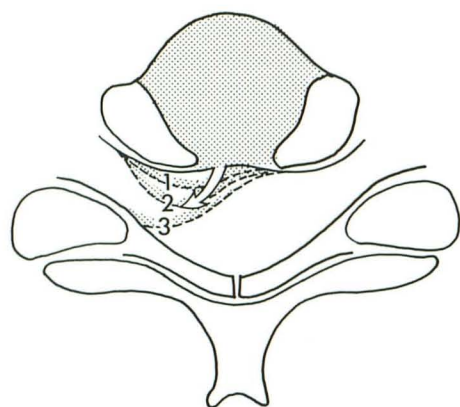
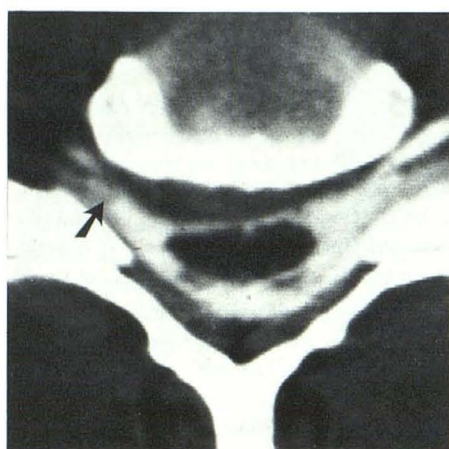
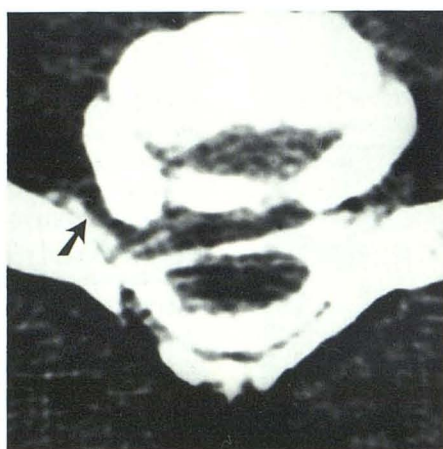


Fig. 7.—Possible evolution of herniated disk. Schematic drawing (A) depicts several stages of disk bulging or disk herniation, indicated by interrupted lines 1–3. These stages are shown on CT myelograms (B–D). Stages 1 (B) and 2 (C) were interpreted as unilateral bulging disks that left corresponding intervertebral foramen more or less open with opacification of root sleeve (arrows). Accordingly, these cases were classed in group 1. Soft mass in stage 3 (D) completely occluded intervertebral foramen and, hence, was interpreted as herniated disk belonging to group 4. A gradual progression from stage 1 to stage 3 is suggested.

A



B



C



D

TABLE 1: Results of Measurements of Cord and Intradural Space at Level of Maximum Pathology

	Group No.			
	2A	2B	1	5
No. of men	9	10	12	18
No. of women	2	3	4	10
Total	11	13	16	28
Mean age (years)	55	45	46	45
AP cord diameter (mm)	4.8	6.3	6.4	7.1
Transverse cord diameter (mm)	13.1	13.9	14.5	13.8
Ratio AP/transverse cord diameter (×100)	37	44	44	51
Cross-sectional cord area in mm ² (SD)	50 (17)	71 (13)	77 (8)	84 (10)
AP diameter of intradural space (mm)	7.2	8.6	10.7	11.9
Cross-sectional area of intradural space in mm ² (SD)	100 (29)	132 (37)	188 (29)	208 (42)
Cross-sectional area of SAS around cord in mm ² (SD)	50 (20)	61 (27)	111 (43)	124 (43)
Ratio cord area/intradural space area (×100)	50	55	41	42

Note.—Group 2A = stenosis with long tract signs; group 2B = stenosis without long tract signs; group 1 = cord deformation in wide canal; group 5 = no cord deformation (all measurements were obtained at C5–C6). The level of maximum pathology in groups 1 and 2 was found at C5–C6 in 66%, at C6–C7 in 28%, and at other levels in 6%. AP = anteroposterior; SAS = subarachnoid space.

prudent to conclude that although group 1 radiologic findings lack specificity, they may have significance if the clinical symptoms are on the same side.

In group 5 (no cord or nerve-root deformity), 18 individuals had unilateral nerve-root symptoms. Symmetric, bilateral, an-

terior bony encroachment upon the dural sac was seen in 10 of these cases, however. Likewise, in group 2B (cord deformation in a narrowed subarachnoid space without long tract signs), the spinal canal nearly always showed concentric narrowing. Nerve-root signs, however, were almost invariably

TABLE 2: Statistical Findings among Groups of Degenerative Disorders of the Cervical Spine

	Correlations between Groups (<i>p</i> values)					
	1/2A	1/2B	1/5	2A/2B	2A/5	2B/5
Mean age	0.05	0.04	0.04	...
AP diameter of cord	0.004	...	0.001	0.01	0.00	0.01
Transverse diameter of cord	0.01	...	0.07
Ratio AP/transverse diameter of cord	*	...	0.01	0.02
Cross-sectional area of cord	0.00	...	0.02	0.004	0.00	0.004
AP diameter of intradural space	0.00	0.00	0.01	0.03	0.00	0.00
Cross-sectional area of intradural space	*	*	0.00	0.00
Cross-sectional area of SAS around cord	0.04	0.05	0.00
Degrees of freedom for the Student <i>t</i> -test	25	27	42	22	37	39

Note.—Only *p* values less than 0.05 from two-tailed *t* tests (except age, which was tested one-tailed) are shown. The degrees of freedom refer to a pooled variance estimate, assuming equal variances in both groups. If necessary, a separate variance estimate was used and degrees of freedom were calculated accordingly. All calculations were performed on a PDP 11-70 computer with SPSS [6]. AP = anteroposterior; SAS = subarachnoid space.

* Testing was not relevant.

TABLE 3: CT Myelographic Features “Specific” for Clinical Nerve-Root Involvement

Group	CT Myelographic Findings	No. of Cases (n = 67)
2B	Stenosis alone	8
2B + 3	Stenosis + root swelling	1
2B + 4	Stenosis + disk herniation	3
3	Root swelling alone	6
3 + 1	Root swelling + cord deformation	1
3 + 4	Root swelling + disk herniation	3
4	Disk herniation alone	3
Total		25

Note.—Patients with long tract signs with or without nerve-root symptoms are not included in this table.

unilateral (11 of 12 cases). Unilateral nerve-root signs in the presence of bilateral narrowing of the spinal canal would appear to argue against a causal relation. On the other hand, literature reports indicate that nerve-root signs may be the precursor of long tract signs in developing spondylotic myelopathy. It is our experience that such nerve-root symptomatology may disappear completely after surgical decompression of the cord. Therefore, lateralization of symptoms may be the result of a minute asymmetry in an apparently symmetric lesion.

A 100% correlation was found between the side of nerve-root symptoms and that of disk herniation, as evidenced by an occluding mass at the entrance on the intervertebral foramen (group 4). This means that such an occluding mass is probably a reliable radiologic sign of local nerve-root compression. The three characteristics of the mass—(1) exclusively composed of soft tissue; (2) completely occluding the entrance of the intervertebral foramen; and (3) extending upward or downward into the lateral recess alongside a pedicle—indicate that it represents a herniated disk. As is evident from the CT myelograms (fig. 6), the mass is in continuation with the intervertebral disk between the uncovertebral joints. It was never seen to bulge maximally in the midline, but always deviated laterally in the direction of the

intervertebral foramen. Perhaps the three cases of soft unilateral mass included in group 1 represent first stages in the development of disk herniation (fig. 7).

In this context it is interesting to note that complete occlusion of the foraminal entrance was never noted in cases with spondylotic encroachment (group 1). Therefore, it appears that only a soft-tissue mass (disk herniation), whether or not in combination with local spondylosis, can compress the nerve root in the lateral region of the spinal canal at the foraminal entrance. More distal compression within the foramen is discussed below.

Nerve-root swelling (group 3) appears to be positively correlated with the side of clinical nerve-root involvement, albeit less strongly than an occluding mass at the foraminal entrance. Characteristically it is limited to the lateral part of the visible segment of nerve root. The more proximal medial part was never included in the swelling. This seems to indicate that the cause of nerve-root swelling must be found immediately distal to the swollen segment, that is, in the intervertebral foramen, or, in case of disk herniation, at the entrance of the foramen.

It is tempting to speculate on the role of foraminal lesions in causing nerve-root compression and swelling. The intervertebral foramina, however, fall outside the scope of our CT myelography study, as only in a few cases does filling of long root sleeves permit demonstration of the nerve root within the foramen. Assessment of the bony dimensions of the foramen does not clarify the problem, as it has long been known that the incidence of bony foraminal narrowing in symptomatic and asymptomatic patients is the same [9]. Possibly intravenously enhanced CT studies of the foramina may be helpful, with unilateral occlusion of the uncinata vein within the foramen indicating nerve-root compression at the same location [10].

Table 3 shows the distribution of CT myelographic features in 25 individuals with clinical nerve-root symptoms only (no long tract signs). Note that some exhibit more than one of these features. We regard the CT myelographic features mentioned in this table as “specific” for clinical nerve-root involvement, including stenosis, because decompression may

have a favorable effect on root symptoms. The other 37 individuals in our group with clinical nerve-root symptoms only exhibited "nonspecific" CT myelographic features, such as unilateral flattening of the cord or no abnormalities. Thus, CT myelographic findings "specific" for clinical nerve-root involvement occurred in 25 (40%) of 62 of these patients.

If we now turn to the spinal cord, it is striking that the significant degree of deformation of the cord in groups 1 and 2B has no detectable clinical significance, as long tract signs are absent. Besides deformation, however, the mean cross-sectional area of the cord in these groups is reduced when compared with the reference group 5 (reduction by 8% and 15%, respectively, tables 1 and 2).

Evidently this degree of cord involvement is not sufficient to produce long tract signs. Such signs do become manifest in group 2A, in which the mean cross-sectional area of the cord has been reduced even more markedly (reduction by 40% compared with group 5). This seems to indicate that the critical value below which long tract signs become manifest lies somewhere between the mean cross-sectional areas of group 2B (71 mm²) and 2A (50 mm²), or somewhere around 60 mm² or 30% reduction in cross-sectional area. The "normal" group 5 indeed contains no individuals with a cross-sectional cord area of less than 60 mm², and in group 1 only one of 16 individuals without long tract signs had a smaller area (54 mm²). In group 2B, two of 12 individuals without long tract signs had smaller areas of 58 and 56 mm², respectively.

In the concentric cord compression present in group 2, it seems likely that the cord may escape loss of function in the early stages by adaptation of its shape to that of the narrowing spinal canal. When loss of cord volume does occur, this need not at first lead to loss of function, a phenomenon comparable to adaptation of the brain to progressive hydrocephalus or a slowly-growing meningioma. After the reduction of cross-sectional cord area has exceeded a critical degree (about 30%) and the remaining cord area has reached a certain minimum (about 60 mm²), decompensation will occur because no more cord volume can be sacrificed without damage to the long tracts. In this connection it is interesting to note that the mean age in groups with long-tract signs (group 2) is 10 years older than in group 2B without such long-tract signs (tables 1 and 2).

It is also worth noting that the cross-sectional area of the subarachnoid space has already been markedly reduced in group 2B (as compared with group 5). This indicates that concentric compression of the cord due to critical reduction of the surrounding subarachnoid space has already started in group 2B.

A recent literature report [5] describes good surgical results in patients with cervical myelopathy and a cord-to-subarachnoid space ratio (cord area divided by total intradural area \times 100) greater than 50, as opposed to poor results in patients in whom the same ratio was less than 50. In the latter group, with a relatively roomy subarachnoid space surrounding an atrophic spinal cord, poor surgical results may indicate that the cord problem is not due to concentric compression, or that cord atrophy, originally the result of concentric compression, has exceeded a critical limit and is now progressing

autonomously. As table 1 indicates, the mean cord-to-subarachnoid space ratio in group 2A is 50. Five patients in this group had a ratio less than 50 and a mean cross-sectional area of the cord of 44 mm². In the other six patients the ratio was more than 50 and the cross-sectional area of the cord had a mean value of 64 mm². Thus, in the patients with a ratio of less than 50, cord atrophy seems to be more pronounced. Table 1 also shows ratios of 41 and 42, respectively, in groups 1 and 5. One should be aware that these low ratios are due to a roomy subarachnoid space and not to cord atrophy (cross-sectional areas of the cord being well over 60 mm²).

Are the values given in table 1 for group 5 (normal appearance of cord and nerve roots) normal? To answer this question we compared the values with data in the literature. In anatomic specimens Elliot [11] measured a cross-sectional area of the cord at the girth of maximal enlargement of 75–85 mm². According to Nordqvist [12], the anteroposterior diameter of the subarachnoid space averages 11.7 mm, with a spread of 9–14 mm. Cord ratio is given by Elliot as 0.58, anteroposterior and transverse diameters of the cord averaging 7.7 and 13.2 mm. According to Di Chiro and Fisher [13], the ratio at C5 is 0.62, the cord diameters averaging 8.5 and 14 mm. All these values are in fair agreement with the data of group 5, the cord in this group 5 having the same cross-sectional area but being slightly flatter in shape.

Comparing the results of CT myelography with those of conventional myelography, we see that the latter studies were always initially judged as normal in groups 1 and 5, but in retrospect sometimes slight loss of density at the involved root sheath could be detected in group 1. In our opinion the findings of CT myelography in group 1 do not add to a better understanding of the clinical picture because they are usually clinically irrelevant. The same is true for group 5, in which conventional myelograms are also normal, minor asymmetry of filling of root sleeves and anterior dural indentations being accepted as insignificant [1].

In groups 2–4, the conventional myelogram was always abnormal. In group 2A, a block in extension or marked anterior and/or posterior indentations of the contrast column were present. Abnormalities in group 3 occasionally proved to be minor, but had been judged invariably as abnormal. Group 4 presented gross abnormalities at the level of the foraminal mass in all cases. Additional information provided by CT myelography in all these groups proved to be relevant. In group 2 deformation of the cord was demonstrated on CT myelography, and measurements of the cross-sectional area of the cord and subarachnoid space contributed to preoperative evaluation. The cause of the concentric compression (spondylotic mass, herniated disk) could be better analyzed. In group 3 sometimes a cause for the nerve-root swelling could be detected (herniated disk, stenosis). In group 4, demonstration of the herniated disk contributed to the preoperative evaluation. In conclusion, we may state that a normal conventional myelogram appears to make a postmyelographic CT investigation superfluous. CT investigation in these cases may even lead to false-positive interpretation of clinically irrelevant findings. In abnormal conventional myelo-

grams, however, additional CT investigation is likely to provide additional information.

In some instances, swollen roots on CT myelography were misinterpreted as herniated disk, especially if they nearly filled the entrance of the foramen. By manipulation of window and level the slight differences in density between the roots and surrounding subarachnoid space can be enhanced, and it will become evident that we are dealing with swollen roots and not with a herniated disk. Another criterion in differentiation of both conditions is that swollen nerve roots occupy only one or two thin adjacent CT slices, while a herniated disk extends axially over larger distances (e.g., 10 or 15 mm or more).

REFERENCES

1. Fox AJ, Lin JP, Pinto RS, Kricheff II. Myelographic cervical nerve root deformities. *Radiology* **1975**;116:355-361
2. Scotti G, Scialfa G, Pieralli S, Boccardi E, Valsecchi F, Tonon C. Myelopathy and radiculopathy due to cervical spondylosis: myelographic-CT correlations. *AJNR* **1983**;4:601-603
3. Nakagawa H, Okumura T, Sugiyama T, Iwata K. Discrepancy between metrizamide CT and myelography in diagnosis of cervical disk protrusions. *AJNR* **1983**;4:604-606
4. Daniels DL, Grogan JP, Johansen JG, Meyer GA, Williams AL, Haughton VM. Cervical radiculopathy: computed tomography and myelography compared. *Radiology* **1984**;151:109-113
5. Badami JP, Norman D, Barbaro NM, Cann CE, Weinstein PR, Sobel DF. Metrizamide CT myelography in cervical myelopathy and radiculopathy: correlation with conventional myelography and surgical findings. *AJNR* **1985**;6:59-64, *AJR* **1985**;144:675-680
6. Nie NH. *Statistical package for the social sciences*. New York: McGraw-Hill, 1975.
7. Sobel DF, Barkovich AJ, Munderloh SH. Metrizamide myelography and postmyelographic computerized tomography: comparative adequacy in the cervical spine. *AJNR* **1984**;5:385-390
8. Hirsch C, Nachemson A. The reliability of lumbar disc surgery. *Clin Orthop* **1963**;19:189-195
9. Friedenbergs ZB, Miller WT. Degenerative disc disease of the cervical spine. *J Bone Joint Surg [Am]* **1963**;45:1171-1178
10. Heinz ER, Yeates A, Burger P, Drayer BP, Osborne D, Hill R. Opacification of epidural venous plexus and dura in evaluation of cervical nerve roots: CT technique. *AJNR* **1984**;5:621-624
11. Elliot HC. Cross-sectional diameters and areas of the human spinal cord. *Anat Rec* **1945**;93:287-293
12. Nordqvist L. The sagittal diameter of the spinal cord and subarachnoid space in different age groups: a roentgenographic post-mortem study. *Acta Radiol [Suppl]* (Stockh) **1964**;227:1-96
13. Di Chiro G, Fisher RL. Contrast radiography of the spinal cord. *Arch Neurol* **1964**;11:125-143